remote sensing

MDPI

Article

Impacts of Arc Length and ECOM Solar Radiation Pressure Models on BDS-3 Orbit Prediction

Ran Li [1,2,*], Chunmei Zhao [3], Jiatong Wu [4], Hongyang Ma [5], Yang Zhang [2], Guang Yang [2], Hong Yuan [2] and Hongyu Zhao [6]

[1] State Key Laboratory of Geo-Information Engineering and Key Laboratory of Surveying and Mapping Science and Geospatial Information Technology of MNR, Chinese Academy of Surveying and Mapping, Beijing 100830, China
[2] Aerospace Information Research Institute (AIR), Chinese Academy of Sciences (CAS), Beijing 100094, China
[3] Institute of Geodesy and Geodynamics, Chinese Academy of Surveying and Mapping, Beijing 100830, China
[4] Map Supervision Center, Ministry of Natural Resources, Beijing 100830, China
[5] School of Geomatics Science and Technology, Nanjing Tech University, Nanjing 210037, China
[6] Logistics Department, Space Systems Division, Beijing 100193, China
* Correspondence: liran@aircas.ac.cn

Abstract: The BeiDou global navigation satellite system (BDS-3) has already provided worldwide navigation and positioning services for which the high-precision BDS-3-predicting orbit is the foundation. The arc length of the observed orbits and the solar radiation pressure (SRP) are two important factors for producing precise orbit predictions. The contribution studies the influences of these factors on BDS-3 orbit prediction. Three-month data from 1 July 2021 to 30 September 2021 are used to analyze optimal arc lengths and different ECOM SRP models for obtaining precise BDS-3 orbit predictions. The results show that the best-fitting arc length for the BDS-3 MEO/IGSO satellite is 42–48 h by comparing the final precise ephemeris and SLR validation. Furthermore, the ECOM9 SRP model shows improved orbit-prediction accuracy than that of the ECOM5 SRP model when the satellites move in and out of the eclipse season. As for the ECOM9 SRP model, the user range error (URE) accuracy of 6 h orbit predictions when satellites are in and outside of the eclipse season is 0.036 m and 0.030 m, respectively. In addition, the orbit prediction accuracy of the BDS-3 satellites does not decrease significantly since BDS-3 satellites apply the continuous yaw-steering (CYS) attitude mode during the eclipse season.

Keywords: BDS-3; precise orbit prediction; satellite laser ranging; eclipse season; ECOM solar radiation pressure model

Citation: Li, R.; Zhao, C.; Wu, J.; Ma, H.; Zhang, Y.; Yang, G.; Yuan, H.; Zhao, H. Impacts of Arc Length and ECOM Solar Radiation Pressure Models on BDS-3 Orbit Prediction. *Remote Sens.* **2022**, *14*, 3990. https://doi.org/10.3390/rs14163990

Academic Editor: Xiaogong Hu

Received: 18 July 2022
Accepted: 12 August 2022
Published: 16 August 2022

1. Introduction

On 23 June 2020, with the successful launch of the last BeiDou global navigation satellite, the BeiDou global navigation satellite system (BDS-3) was fully completed and includes three geostationary earth orbit (GEO) satellites, three inclined geosynchronous orbit (IGSO) satellites, and twenty-four medium earth orbit (MEO) satellites [1]. BDS-3 can provide global services, such as positioning, velocity, and timing with accuracies of 10 m, 0.2 m/s, and 20 ns, respectively. Since the satellite orbit is the foundation for high-precision services and applications of BDS-3 [2], any global navigation satellite system (GNSS) error will directly affect the accuracy of navigation and positioning solutions, e.g., the emergence of real-time precise point-positioning real-time kinematic (PPP-RTK) technology [3], real-time atmospheric monitoring [4,5], early GNSS-based earthquake warning, and other technologies [6–9]. Therefore, precise real-time GNSS satellite orbits are urgently required for scientific and industrial communities. International GNSS Service (IGS) ultra-rapid (IGU) orbits are always implemented in BDS-3 real-time applications [10], and each IGU orbit product contains the observed orbits of the first 24 h, as well as the predicted orbits of

the next 24 h. However, only certain parts of the predicted orbits are useful for real-time users since the IGU orbits are updated every 6 h with a latency of 3 h. Therefore, it is essential to study BDS-3-predicted orbits. The accuracy of the predicted orbits depends on the accuracy of the initial satellite conditions (satellite position and velocity at the initial epoch) and the accuracy of the solar radiation pressure (SRP) models [11].

The initial conditions of the satellite are affected by the fitted arc length of the observed orbit, and the satellite orbits are then predicted based on the initial conditions. Choi et al. (2013) studied Global Positioning System (GPS) ultra-rapid orbit-prediction strategies and found that the optimal arc length of the observed orbits is around 40–45 h [11]. Li et al. (2015) assessed the impact of the arc length on GPS precise point position (PPP) solutions [12], and the results showed that the highest PPP ambiguity fix rates can be achieved when using predicted orbits with an arc length of 42 h. Geng et al. (2018) analyzed the effect of the arc length of the observed orbits on multi-GNSS orbit prediction performances [13], and they found that the optimal arc length is 42–45 h. The optimal arc lengths for predicting orbits of GPS, GLONASS, BDS-2, and GALILEO satellites have been studied for many years; however, few existing manuscripts involve the same research effort for the BDS-3 satellites. How the accuracy of the BDS-3 predicted orbits varies with the arc length of the observed orbit needs to be uncovered. Therefore, it is necessary to study the optimal fitting arc length for BDS-3-predicted orbits.

As one of the major error sources of satellite orbit determination, solar radiation pressure model errors significantly affect the precision of precise satellite orbit determination and prediction [14,15]. Numerous studies have conducted research on the SRP model of GNSS satellites [16–18]. However, the research on the SRP model is limited to precise orbit determination, and few are related to precise orbit prediction. The accuracy of GPS satellites could decrease to 300 m in 3 days because of the existence of solar radiation pressure perturbations [19]. Therefore, investigating different solar radiation pressure models in orbit prediction is necessary. Although the ECOM SRP model is a widely used SRP model in precise GNSS orbit determination [18], the ECOM SRP model is designed for GPS satellites, and its applicability to BDS-3 satellite orbit prediction needs to be further verified. Therefore, this article will concentrate on the impact of the ECOM SRP model on BDS-3 satellite orbit prediction.

The BDS MEO satellites enter the eclipse season twice a year, each time lasting 8–15 days [20]. If this study does not consider the eclipse season and only investigates satellite orbit-prediction accuracies in the non-eclipse season, all orbit prediction starting times are outside the eclipse season. Hence, orbit prediction times are extended to 8–15 days, which would significantly reduce the prediction accuracy of the satellite orbit. Therefore, it is worthy to study the prediction accuracy of BDS-3 satellite orbits during the eclipse season. The China Satellite Navigation Office (CSNO) released BDS-3 satellite metadata in 2019, announcing that the BDS-3 MEO/IGSO satellites adopt continuous yaw steering (CYS) attitude modes during eclipse seasons [18]. The accuracy of current GNSS satellite orbits is significantly degraded during eclipse seasons, particularly for long-arc solutions and orbit predictions [21]. Duan et al. (2019) pointed out that the reason for such degradations is primarily due to the ignorance of thermally imbalanced forces [22]. Xia et al. (2022) also found that orbit degradations result from the unaccounted non-conservative forces, e.g., thermal radiation during Earth's shadow transitions [23]. The above studies are all based on the precise orbit determination of the BDS-3 satellites, and the study of the orbit prediction accuracy of the BDS-3 satellites during the eclipse season is essential as well.

This contribution mainly studies the impact of the arc length and ECOM SRP models on BDS-3 orbit prediction. The article is organized as follows. We first introduce the orbit-prediction method and the experimental data in Section 2. Afterward, the final precise ephemeris and SLR data were used to evaluate BDS-3's orbit prediction accuracy by using different arc lengths in Sections 3.1 and 3.2, and the orbit prediction accuracy of the BDS-3 satellites during and outside of eclipse seasons is provided in Section 3.3. Additionally, we analyze the impact of different ECOM SRP models on the predicted orbit accuracy of

the BDS-3 satellites in Section 3.4. Finally, discussions and conclusions are provided in Sections 4 and 5.

2. Orbit Prediction Method and Data Collection

2.1. Orbit Prediction Method

Satellite orbit prediction accuracy relies on the satellite's initial conditions and solar radiation pressure parameters. Hence, in the following paragraph, we will indicate the solution of the satellite's initial conditions and solar radiation pressure parameters over an arc period using the least-squares method.

Let the position, velocity, and dynamic parameters of the satellite at the initial time t_0 be $(r_0, \dot{r}_0, p_0)$. By considering the influence of various perturbation forces, the position and velocity $(r, \dot{r})$ of the satellite at epoch t can be obtained by integrating the satellite dynamics equation. We can predict the satellite orbit at the epoch t as follows:

$$(r, \dot{r}) = F(t, r_0, \dot{r}_0, p_0) \tag{1}$$

where F is the nonlinear integral function. The observation equation can be described by Equation (2):

$$r_t - r = \Phi(t, t_0)\begin{bmatrix}\Delta r_0 & \Delta \dot{r}_0 & \Delta p_0\end{bmatrix}^T \tag{2}$$

where $\Phi(t, t_0) = \begin{bmatrix}\frac{\partial r}{\partial r_0} & \frac{\partial r}{\partial \dot{r}_0} & \frac{\partial r}{\partial p_0}\end{bmatrix}$ is the state transition matrix; $\Delta r_0, \Delta \dot{r}_0, \Delta p_0$ denote the correction value of the initial position, velocity, and dynamic parameters, respectively.

Assuming that the satellite position at the epoch t_i in the precise ephemeris is r_i during an arc length $[t_i, t_m]$, the m-dimensional observation equation can then be constructed as follows:

$$Y = \theta(\Delta r_0, \Delta \dot{r}_0, \Delta p_0) \tag{3}$$

where the following is the case.

$$Y = \begin{bmatrix} r_{t_1} - r_1 \\ r_{t_2} - r_2 \\ \vdots \\ r_{t_m} - r_m \end{bmatrix}$$

$$\theta(\Delta r_0, \Delta \dot{r}_0, \Delta p_0) = \begin{bmatrix} \theta_1(\Delta r_0, \Delta \dot{r}_0, \Delta p_0) \\ \theta_2(\Delta r_0, \Delta \dot{r}_0, \Delta p_0) \\ \vdots \\ \theta_m(\Delta r_0, \Delta \dot{r}_0, \Delta p_0) \end{bmatrix} = \begin{bmatrix} \Phi(t_1, t_0)\begin{bmatrix}\Delta r_0 & \Delta \dot{r}_0 & \Delta p_0\end{bmatrix}^T \\ \Phi(t_2, t_0)\begin{bmatrix}\Delta r_0 & \Delta \dot{r}_0 & \Delta p_0\end{bmatrix}^T \\ \vdots \\ \Phi(t_m, t_0)\begin{bmatrix}\Delta r_0 & \Delta \dot{r}_0 & \Delta p_0\end{bmatrix}^T \end{bmatrix}$$

The satellite's position, velocity, and dynamic parameters at the initial epoch t_0 can be calculated by applying least-squares estimations in Equation (3). Finally, the predicted orbits are generated through orbit integration using precise satellite initial conditions.

2.2. Data Collection and Dynamic Model

The final orbit products released by the Center for Orbit Determination in Europe (CODE) are used for BDS-3 orbit prediction research studies, and the data's length ranges from 1 July 2021 to 30 September 2021. The final precise ephemeris is not only used as observed orbits but also as reference orbits for evaluating the accuracy of BDS-3-predicted orbits. Table 1 summarizes the precise orbit-prediction strategies in the experiment, including the dynamical models and integration method. It is noteworthy that in order to reduce the influence of Earth orientation parameter (EOP) errors on the predicted orbit, this study uses the final EOP released by the IERS Earth orientation center. Moreover, the same empirical force parameters, integration methods, and integration step sizes are used in this experiment.

Table 1. Dynamical models and integration method.

Models	Reference/Source
Geopotential	EGM 2008, 12 × 12 degree [24]
N-body gravitation	JPL DE405 ephemeris [25]
EOP	Fixed to IERS EOP 14 C04 dataset
SRP model	ECOM5 model, ECOM7 model, ECOM9 model
Solid earth tides, pole tides	IERS conventions 2010 [26]
Ocean tides	FES2004 [27]
Relativity effect	IERS2010
Integration	Collocation Integration method
Integration step size	900 s

As can be seen on the website of the precise orbit-determination strategies adopted by the major analysis centers of IGS (see https://files.igs.org/pub/center/analysis/, accessed on 17 January 2022), most analysis centers use nine-parameter ECOM or its simplified version to determine precise orbits [28]. Therefore, ECOM and its simplified version were used in our BDS-3 orbit prediction strategy to assess its accuracy in orbit prediction. The ECOM SRP model adopts the form of constant components in addition to periodic terms. Three sets of parameters were used to absorb the influence of solar radiation pressure [29]. The ECOM SRP model formulas are as follows:

$$\begin{aligned} \vec{a} &= a_{srp,D} \cdot \vec{e_D} + a_{srp,Y} \cdot \vec{e_Y} + a_{srp,B} \cdot \vec{e_B} \\ a_{srp,D} &= D_0 + D_{Cu} \cos u + D_{Su} \sin u \\ a_{srp,Y} &= Y_0 + Y_{Cu} \cos u + Y_{Su} \sin u \\ a_{srp,B} &= B_0 + B_{Cu} \cos u + B_{Su} \sin u \end{aligned} \tag{4}$$

where $\vec{a}$ represents the acceleration of SRP, $a_{srp,D}$, $a_{srp,Y}$, $a_{srp,B}$ are the SRP accelerations of the D-axis, Y-axis, and B-axis, respectively. u is the argument of the ascending node, and D_0, D_{Cu}, D_{Su}, Y_0, Y_{Cu}, Y_{Su}, B_0, B_{Cu}, and B_{Su} are constant parameters, which are estimated in the orbit's determination process. In the following, when these nine parameters are used for parameter estimations, we call this strategy the ECOM9 SRP model. Springer et al. (1999) introduced a simplified ECOM SRP model containing only 5 parameters (D_0, B_0, Y_0, B_{Cu}, and B_{Su}) [30], which is called the ECOM5 SRP model. The experimental results confirm that when the ECOM SRP model with 7 parameters (D_0, D_{Cu}, D_{Su}, Y_0, B_0, B_{Cu}, and B_{Su}) is used, the orbit's overlap accuracy with resepct to BDS-2's precise orbit determination can be greatly improved [31], which is called the ECOM7 SRP model in the following.

3. Results and Analysis

The accuracies of BDS-3-predicted orbits with different arc lengths are compared to the IGS final precise orbits and SLR data. Three-month data from 1 July 2021 to 30 September 2021 are used in this experiment. The BDS-3 satellite orbit prediction accuracy during and outside of eclipse seasons is provided. Finally, the impacts of different ECOM SRP models on the predicted orbit accuracy of the BDS-3 satellite are discussed. Because of the poor orbital accuracy of the BDS-3 GEO satellites, the BDS-3 GEO satellites will not be considered in this experiment. It should be noted that in Sections 3.1–3.3, we use the ECOM9 SRP model for orbit prediction.

3.1. Impacts of the Arc Length on Orbit Prediction

The user range error (URE) is used to verify the accuracy of the predicted orbit. The satellite URE is associated with the maximum opening angle of the satellite relative to Earth [15]. Without considering the satellite clock error, the MEO satellites' URE is computed as follows [21]:

$$URE_{MEO} = \sqrt{(0.99\Delta R)^2 + (0.14\Delta T)^2 + (0.14\Delta N)^2} \tag{5}$$

where ΔR, ΔT, ΔN are the radial, along-track, and cross-track components of the satellite orbit, respectively. For IGSO and GEO satellites, URE is computed as follows.

$$URE_{GEO/IGSO} = \sqrt{(\Delta R)^2 + (0.99\Delta T)^2 + (0.99\Delta N)^2} \quad (6)$$

It can be seen from the Formulas (5) and (6) that the most significant contribution to URE is the radial component of the satellite orbit.

The orbit prediction accuracy of BDS-3 MEO satellites is first calculated in the experiment. The 24–72 h satellite-orbit arc lengths are used as initial observation data. IGS's final precise ephemeris is used as the reference. We use the root mean square (RMS) in the radial (R), along-track (T) and cross-track (N) directions and URE to evaluate the accuracy of BDS-3-predicted orbits. The accuracy of the first 6 h and 24 h of predicted orbits is used to evaluate the impact of the arc length on BDS-3 MEO orbit prediction.

As shown in Figure 1, the smallest orbital URE is in the fitted arc length of 42–48 h for both 6 h and 24 h orbit prediction. It can be observed that the accuracy of the radial, along-track, and cross-track are similar to that of the URE, and the best fitting arc length is 42–48 h. The results also show that when the prediction intervals are 6 h, the URE is the smallest at the arc length of 42 h, and the URE, radial, cross-track, and along-track are 0.029 m, 0.019 m, 0.022 m, and 0.054 m, respectively. When the prediction intervals are 24 h, the URE is also the smallest at the arc length of 42 h, and the URE, radial, cross-track, and along-track are 0.051 m, 0.027 m, 0.034 m, and 0.111 m, respectively.

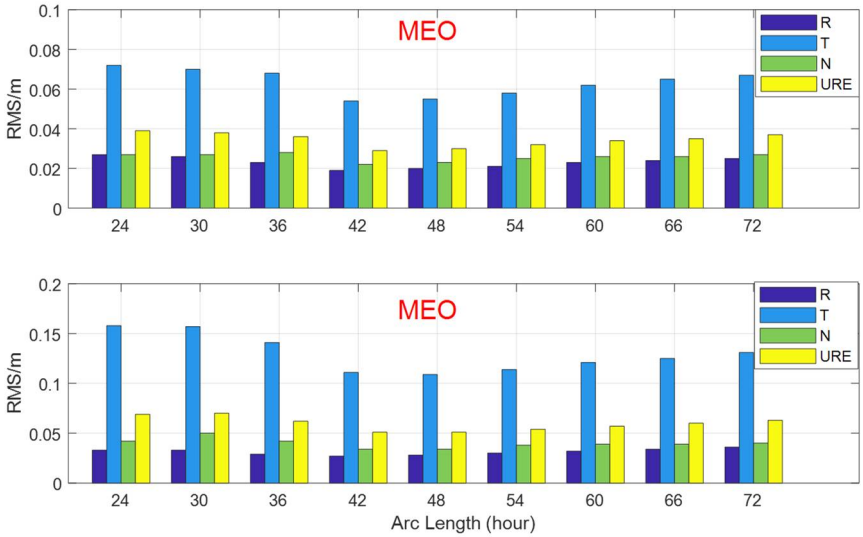

Figure 1. The accuracy of the first 6 h (**top**) and 24 h (**bottom**) of predicted BDS-3 MEO orbits with different arc lengths.

Meanwhile, the orbit prediction accuracy of BDS-3 IGSO satellites is analyzed. BDS-3 has three IGSO satellites (C38, C39, and C40). In this contribution, these BDS-3 IGSO satellites are taken as an example to explore the best-fitting arc length.

As is shown in Figure 2, the results of BDS-3 IGSO are consistent with those of BDS-3 MEO satellites. The smallest orbital URE is in the fitted arc length of 42–48 h for both 6 h or 24 h length orbit prediction. The results show that when the prediction intervals are 6 h, the URE is the smallest at the arc length of 42 h, and the URE, radial, cross-track, and along-track are 0.193 m, 0.125 m, 0.080 m, and 0.125 m, respectively. When the prediction intervals are 24 h, the URE is also the smallest at the arc length of 42 h, and the URE, radial, cross-track, and along-track are 0.231 m, 0.108 m, 0.080 m, and 0.189 m, respectively. It is noteworthy that, compared to BDS-3 MEO satellites, the accuracy of BDS-3 IGSO satellite orbit prediction is significantly reduced when the fitted arc length is less than 36 h. The reason may be that the BDS-3 IGSO satellite has a longer orbital period than the MEO

satellite. Therefore, when the fitted arc length is less than 36 h, the accuracy of BDS-3 IGSO satellite orbit predictions will diminish compared to that of the BDS-3 MEO satellites.

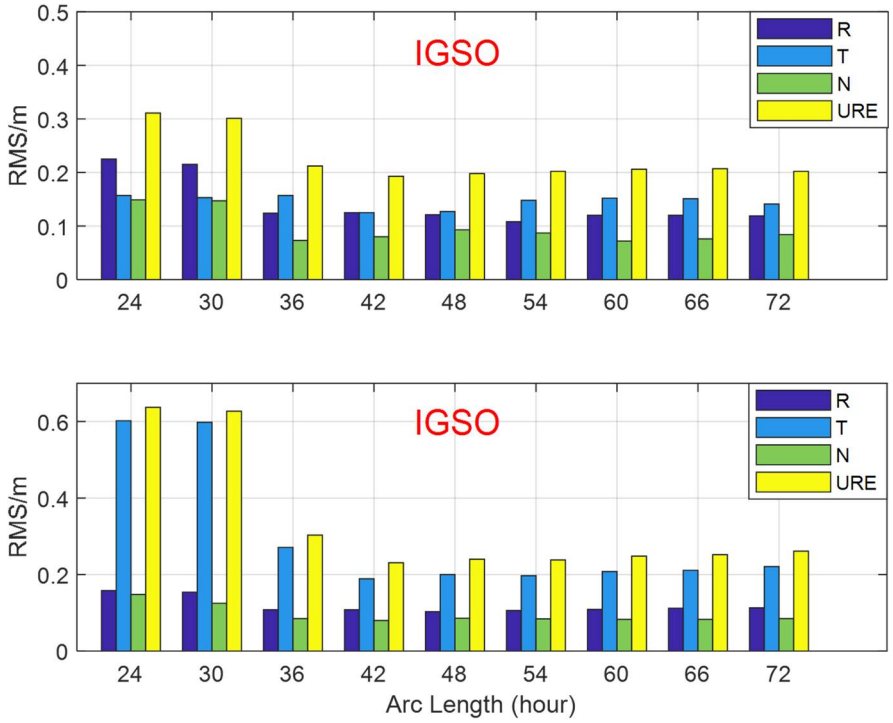

Figure 2. The accuracy of the first 6 h (**top**) and 24 h (**bottom**) of predicted BDS-3 IGSO orbits with different arc lengths.

3.2. Satellite Laser Ranging Validation

Satellite laser ranging is a commonly used method for evaluating orbit accuracy, and its accuracy can reach the millimeter level [32]. Currently, BDS-3 has four MEO satellites (C20, C21, C29, and C30) that are observed by SLR stations coordinated by the International Laser Ranging Service (ILRS). This paper uses the SLR data to verify the BDS-3 satellite's best-fit arc length. The experiment uses three-month SLR data from 1 July 2021 to 30 September 2021. Moreover, we used 24 h predicted orbits for conducting evaluations.

As shown in Figure 3, the best-fitting arc length is 42–48 h for C20, C21, and C30 satellites. The conclusion is consistent with the result of the final IGS precise ephemeris. However, the SLR residual of the C29 satellite is the smallest when the fitting arc is 60 h. It should be noted that the orbit prediction accuracy of the C29 satellite under the fitting arc length of 42–72 h is almost the same as 60 h, with differences within 3 mm.

As is shown in Figure 4, most SLR residuals for BDS-3 satellites are within ±20 cm. There are 361, 287, 238, and 245 normal points for C20, C21, C29, and C30 satellites, respectively. In this paper, the absolute values larger than 50 cm have been removed. After gross error elimination, there are 354, 281, 232, and 227 normal points left; thus, in this experiment, we used more than 96% of the original data for analysis. The accuracy of the predicted orbit is evaluated by SLR, and the RMS values of the SLR residuals for C20, C21, C29, and C30 are 5.36, 5.51, 5.49, and 6.01 cm, respectively. The overall RMS value of SLR residuals for the BDS-3 MEO satellites is 5.59 cm, which shows that the orbital accuracy of the BDS-3 MEO satellites is still maintained at a high level after 24 h of satellite orbit predictions.

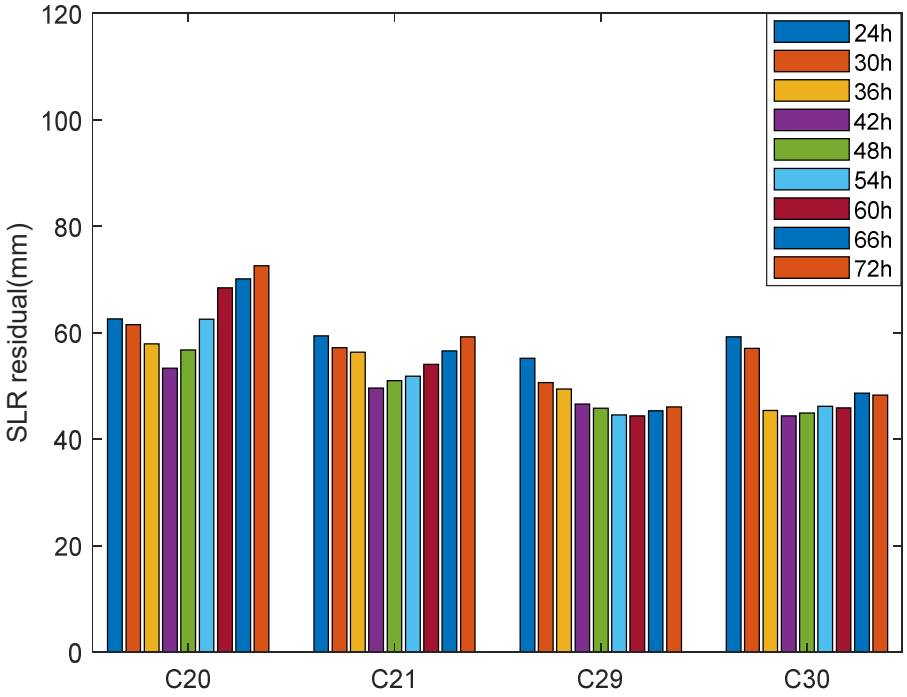

Figure 3. SLR residuals for BDS-3 MEO satellites with different arc lengths.

When the fitting arc length is 42 h, the laser-ranging validation residuals for those four satellites are shown in Figure 4.

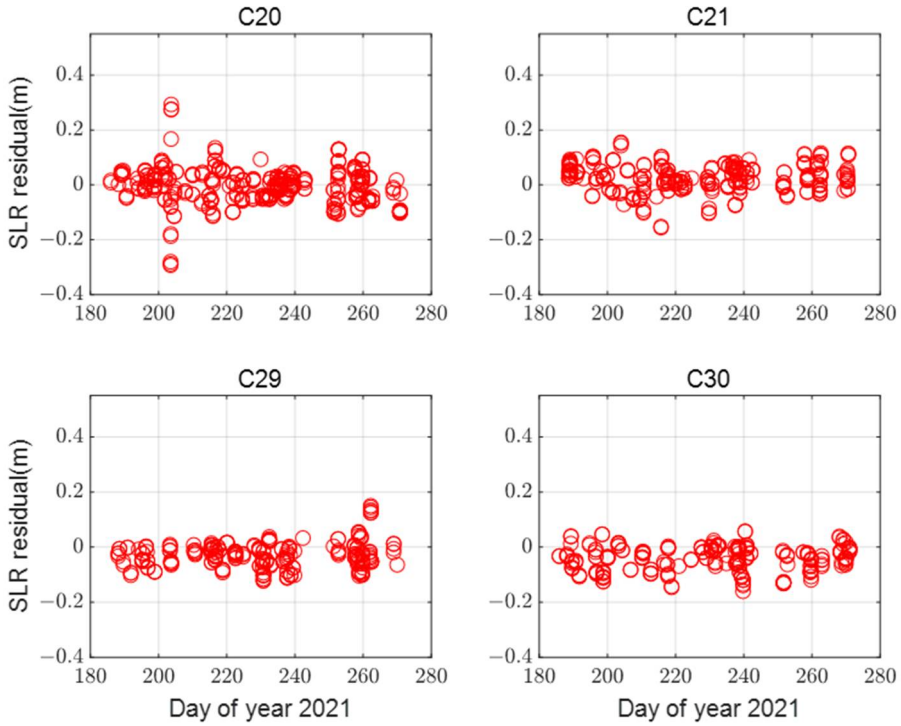

Figure 4. SLR residuals for BDS-3 satellites with prediction interval of 24 h (red circles represent SLR residuals).

3.3. Orbit Prediction Accuracy When Satellites Are during and Outside of Eclipse Season

For the BDS-2 satellite, studies have shown that its orbit determination accuracy will decrease significantly during the eclipse period [20], but there are few studies analyzing the orbit prediction accuracy of the BDS-3 satellite during the eclipse season. Therefore,

in the following section, this study explores the orbit prediction accuracy of the BDS-3 satellite during the eclipse season. The BDS-3 IGSO and MEO satellites enter the eclipse season when the $|\beta|$ angle (the elevation angle of the sun above the orbital plane) is less than 8.7° and 12.97°, respectively [33]. Figure 5 shows the eclipse seasons for the BDS-3 satellites. The period of the BDS-3 satellites during the eclipse season is from 1 July 2021 to 30 September 2021.

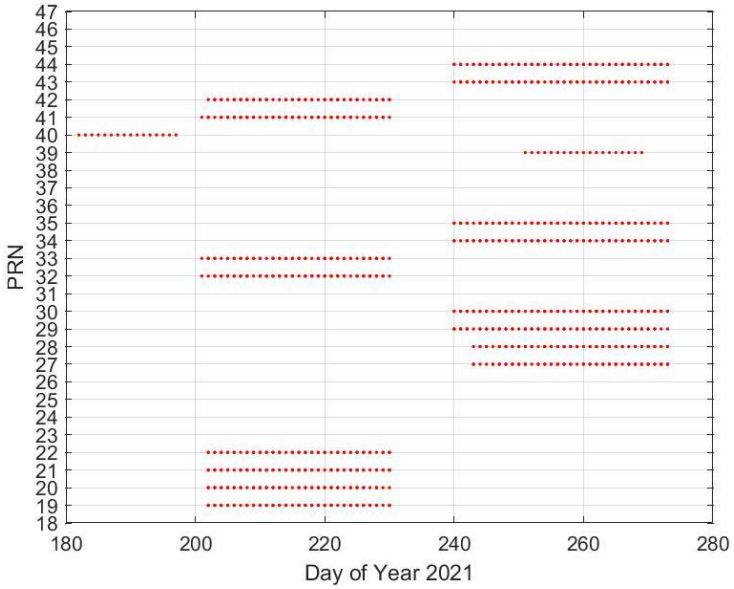

Figure 5. Eclipse seasons for the BDS-3 satellites (1 July 2021 to 30 September 2021, red dots represent eclipse seasons).

As shown in Figure 5, 18 BDS-3 satellites experienced the eclipse seasons during the selected three months. Day of year (DOY) 202 to 230, 2021, was selected, during which eight satellites (C19, C20, C21, C22, C32, C33, C41, and C42) were within the eclipse season. Meanwhile, DOY 243 to 273, 2021 was selected, during which the same eight satellites were outside if the eclipse season. Taking the selected eight BDS-3 satellites as an example, we analyzed the orbit prediction accuracy of BDS-3 satellites using different arc lengths when satellites move in and out of eclipses seasons. It should be pointed out that the selected eight BDS-3 satellites are all MEO satellites. Figure 6 shows the orbit prediction accuracy of different arc lengths when the satellites move in and out of eclipses seasons.

It can be seen from Figure 6 that the arcs of 42–48 h length are the best fitting arc lengths for both satellites moving out of eclipse seasons and those into eclipse seasons. Taking the 48 h fitting arc length as an example, when the prediction intervals are 6 h, the URE increases from 0.0344 m out of eclipse seasons to 0.0419 m during eclipse seasons, which corresponds to an increase of 22%; when the prediction intervals are 24 h, the URE increases from 0.0592 m out of eclipse seasons to 0.0772 m in eclipse seasons, which corresponds to increases of 30%. Compared with the significant decrease in the orbital accuracy of the BDS-2 satellite moving in eclipse seasons, the BDS-3 satellites do not experience a significant decrease in their orbit prediction accuracy. The reason may be due to the advanced attitude control mode of the BDS-3 satellites. In addition to the yaw-steering (YS) mode, the BDS-3 MEO/IGSO satellites adopt the continuous yaw steering (CYS) attitude mode in eclipse seasons [20]. The CYS mode not only meets the requirements of the power supply and thermal control of the BDS-3 MEO/IGSO satellites but also avoids rapid yaw slews near the sun–spacecraft–Earth geometries. The results indicate that the proper attitude mode improved BDS-3's orbit prediction accuracy.

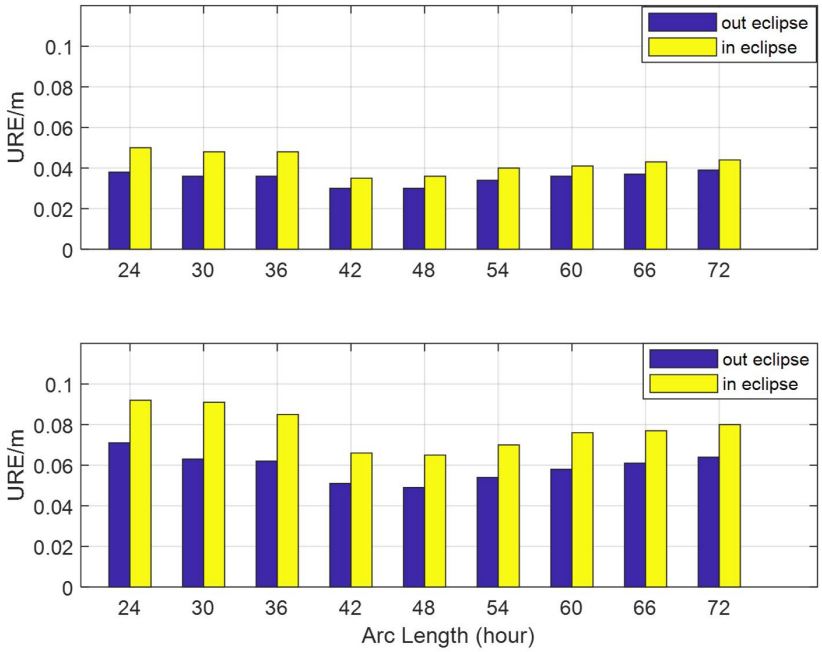

Figure 6. The URE of BDS-3 predicted orbits in and out of eclipse season with prediction intervals of 6 h (**top**) and 24 h (**bottom**).

3.4. Analysis of Different ECOM SRP Models for Orbit Prediction

BDS-3 satellites adopt a different attitude control mode from the BDS-2 satellite. For the BDS-3 MEO/IGSO satellites, the CYS mode is adopted during the eclipse seasons, and the YS mode is adopted out of eclipse seasons.

The BeiDou satellite navigation system has three satellite attitude-control modes: YS mode, orbit-normal (ON) mode, and CYS mode.

The BDS-2 satellite adopts the YS and ON modes. For the YS mode, the satellite uses the solar sensor and the Earth sensor to detect the position of the sun and the Earth; thus, this mode satisfies that requirement in which the satellite antenna points to the center of the earth and the solar panel is always perpendicular to the direction of the sun's illumination. After the BDS-2 IGSO/MEO satellites move into the eclipse season and the β angle (defined by the angle of the sun above the orbit plane) is between -4° and $+4^\circ$, the attitude control mode of the BDS-2 IGSO/MEO satellites changes from the YS mode to the ON mode [34]. As for the ON mode, the yaw angle φ (defined by the angle between the instantaneous velocity and the body-fixed x-axis) is always zero. However, studies have shown that when BDS-2 IGSO/MEO satellites move into the eclipse season, the satellites adopting the ON mode will cause a significant decrease in the accuracy of the satellite's orbit determination [35]. Therefore, the CYS mode is adopted in the BDS-3 MEO/IGSO satellites.

When the BDS-3 MEO/IGSO satellites move in the eclipse season, the satellite adopts the YS and CYS modes. During most of the eclipse season, the BDS-3 MEO/IGSO satellites use the YS mode. The CYS mode includes two periods of midnight-turn maneuver and noon-turn maneuver. Midnight-turn maneuver and noon-turn maneuver are activated when the β angle is between -3° and $+3^\circ$, and the sun's azimuth angle $|\alpha|$ (defined by the angle between Earth-satellite vector and Earth-"noon" vector on the orbit plane) is $\leq 10^\circ$ or $|\alpha \pm 180^\circ| \leq 10^\circ$ [20]. As for the CYS mode, the solar sensor can no longer control the yaw's attitude, and the BDS-3 MEO/IGSO satellites start to yaw with estimated hardware yaw rates in order to make the yaw angle transform 180°. Yaw attitude departs from the nominal values and it can take up to 30 min to 1 h to correct [36]. Compared with the YS mode, the CYS mode adopts the method of starting the maneuver in advance and ending

the maneuver with a delay; thereby, the CYS mode avoids rapid yaw slews near collinear sun–spacecraft–Earth geometries.

The satellite attitude control mode will affect the solar radiation pressure related to the irradiated surface, which will further affect the accuracy of the satellite's precise orbit predictions [37]. Therefore, it is necessary to study the BDS-3 satellite's orbit prediction accuracy for different ECOM SRP models in and out of the eclipse seasons.

Similarly to Section 3.3, eight BDS-3 satellites (C19, C20, C21, C22, C32, C33, C41, and C42) were selected to study the orbital prediction accuracy of the ECOM5, ECOM7, and ECOM9 SRP models when moving in and out of the eclipse seasons.

As shown in Figure 7, the orbit prediction accuracy of the ECOM5, ECOM7, and ECOM9 SRP models is similar in and out of eclipse seasons. The orbital UREs using the ECOM5, ECOM7, and ECOM9 SRP models are 0.035 m, 0.031 m, and 0.030 m outside eclipse seasons, respectively. However, the orbital UREs using the ECOM5, ECOM7, and ECOM9 SRP models are 0.048 m, 0.037 m, and 0.036 m during the eclipse seasons, respectively. The results show that the orbital URE of the ECOM9 model is 19% lower than that of using the ECOM5 SRP model. In addition, the ECOM7 and ECOM9 SRP models show similar orbit prediction accuracy, and both are better than the ECOM5 SRP model. The reason may be that the added parameters absorb more orbital errors.

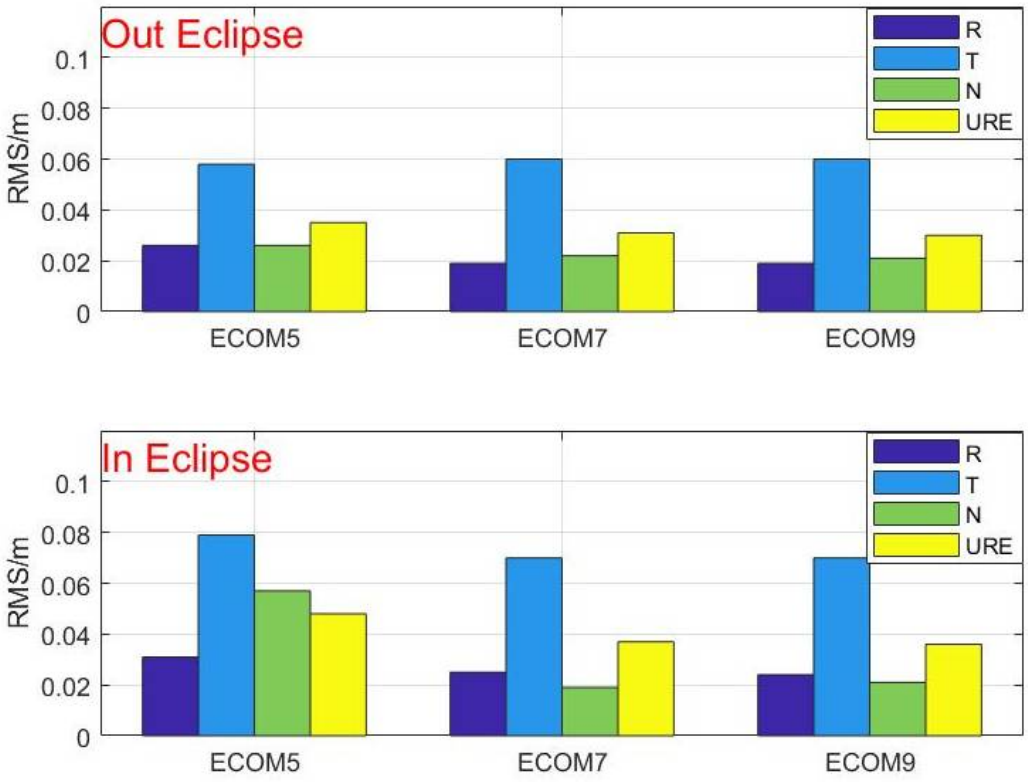

Figure 7. Accuracy of BDS-3 predicted orbits with different ECOM SRP models when satellites move in and out of eclipse seasons (6 h prediction interval).

In addition, we study the orbit prediction accuracy for different ECOM SRP models with different arc lengths. Figure 8 shows the orbit prediction accuracy for different ECOM SRP models out of the eclipse seasons with the prediction interval of 24 h.

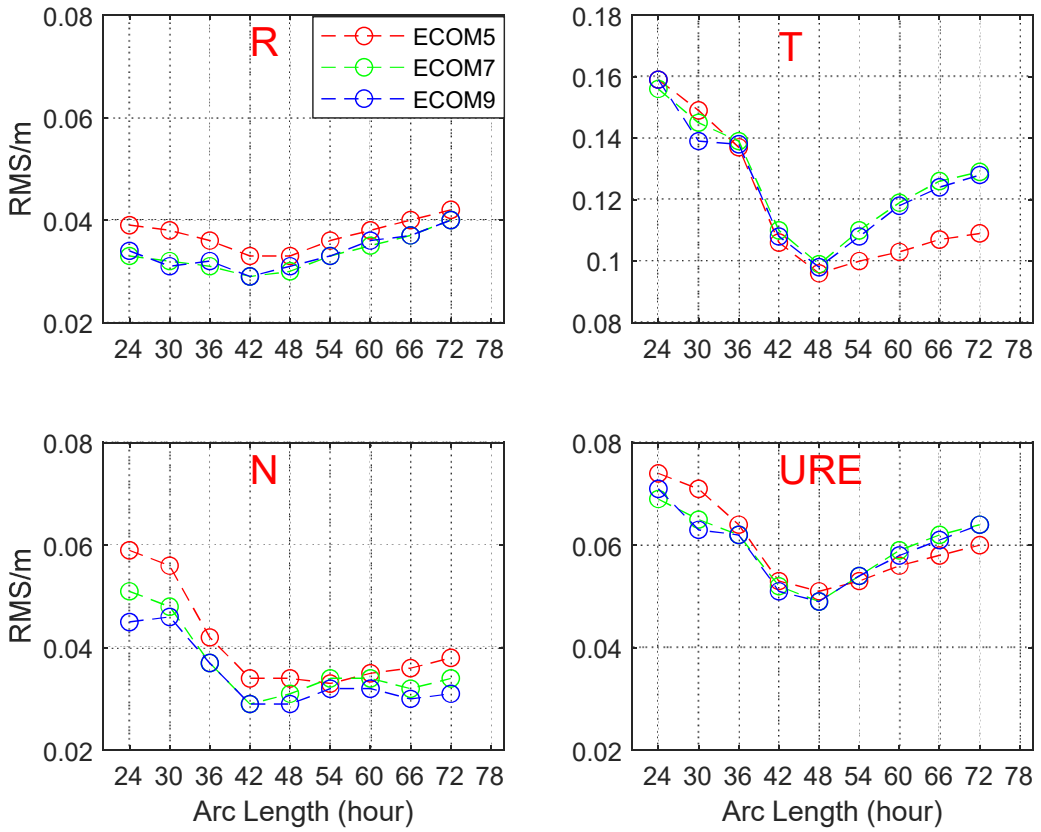

Figure 8. Average RMS and URE of BDS-3 predicted orbits with different ECOM SRP models out of eclipse seasons (24 h prediction interval).

As shown in Figure 8, the optimal arc lengths using the ECOM5, ECOM7, and ECOM9 SRP models are 42–48 h. The difference in orbit prediction accuracy between ECOM7 and ECOM9 SRP models is within 2 mm, and the performances of both ECOM7 and ECOM9 SRP models surpass the ECOM5 SRP model. Moreover, when the fitted arc length is less than 48 h, the orbital accuracy of the ECOM7 and ECOM9 SRP models is better than that of the ECOM5 SRP model. However, when the fitted arc length is longer than 48 h, the ECOM5 SRP model exhibits improved orbit prediction accuracy. The reason is that the ECOM5 SRP model shows improved orbit prediction accuracy in the along-track direction.

Figure 9 shows the orbit prediction accuracy of different ECOM SRP models during the eclipse seasons with the prediction interval of 24 h. The optimal arc lengths using the ECOM5, ECOM7, and ECOM9 SRP models are 42–48 h. The ECOM7 and ECOM9 models have good performances with respect to orbit prediction during the eclipse seasons, for which the orbital UREs are both 0.065 m. However, the orbit prediction accuracy of the ECOM5 SRP model during the eclipse seasons is unsatisfactory, particularly in the cross-track direction. When the arc length is longer than 36 h, the orbit prediction accuracy in the cross-track direction becomes worse, and the cause needs to be further studied. Therefore, using the ECOM9 or ECOM7 SRP model is recommended when performing precise orbit predictions for the BDS-3 MEO satellites during eclipse seasons.

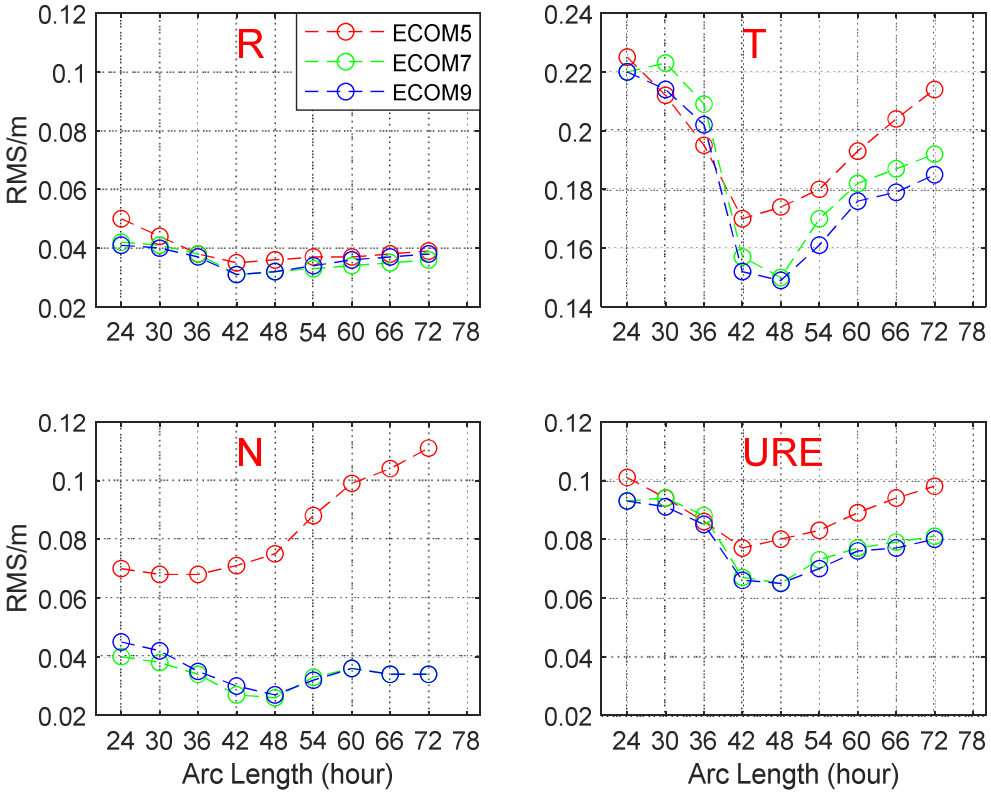

Figure 9. Average RMS and URE of BDS-3 predicted orbits with different ECOM SRP models in eclipse seasons (24 h prediction interval).

4. Discussion

This contribution studies two critical factors (arc length and SRP model) affecting the BDS-3 satellite's orbit-prediction accuracy. We use precise ephemerides and SLR data to verify the BDS-3 satellite's best-fit arc length. Our results show that the best-fitting arc length for the BDS-3 satellites is at 42–48 h. In addition, the BDS-3 satellite's orbit prediction accuracy does not decrease significantly during the eclipse seasons, which should be attributed to the advanced attitude control mode for the BDS-3 satellite. We also find out that the BDS-3 satellite's orbit prediction accuracy of the ECOM5 SRP model during the eclipse seasons is unsatisfactory, especially in the cross-track direction. Therefore, when the BDS-3 satellites are within the eclipse seasons, we recommend using the ECOM9 or ECOM7 SRP model for orbit prediction.

Since the Earth's orientation parameters also have a significant influence on the orbit-prediction accuracy, we will study the use of real-time earth orientation parameters to analyze orbit-prediction accuracies in the future.

5. Conclusions

Three-month data from 1 July 2021 to 30 September 2021 were used to analyze orbit-prediction accuracies under different conditions, including precise ephemerides and SLR data, and to study the effect of arc lengths on orbit-prediction accuracy. We also explore the orbit-prediction accuracy of different ECOM SRP models during and outside of the eclipse seasons. Based on the above results, we can reach the following conclusions.

The final precise ephemerides and SLR validations show that the best-fitting arc length for the BDS-3 satellites is 42–48 h. In contrast to the BDS-3 MEO satellites, the BDS-3 IGSO satellites have diminished orbit-prediction accuracies when the fitting arc length is shorter than 36 h. The result shows that the orbital accuracy of the BDS-3 MEO satellites maintains a high level after 24 h of satellite orbit predictions. The UREs of BDS-3 MEO- and IGSO-predicted orbits are 0.051 m and 0.231 m, respectively. SLR validation shows

that the BDS-3 satellites have the best orbit prediction accuracy for the arc length of 42 h; thus, the average SLR residual is approximately 5.59 cm with a prediction interval of 24 h.

Regardless of whether the satellites are within or outside of the eclipse seasons, the best fitting arc length is 42–48 h. Compared with the BDS-2 satellite's attitude control mode, the BDS-3 satellites adopt the CYS mode, which does not significantly reduce orbit-prediction accuracies during the eclipse seasons. When the arc length is 42 h and the orbit is predicted for 24 h, the UREs of the BDS-3 MEO satellite are 0.077 m and 0.059 m during and outside of the eclipse seasons, respectively.

The experimental results show that the ECOM9 SRP model has the best orbit prediction accuracy during and outside of eclipse seasons. The UREs of the 6 h predicted orbit are 0.036 m and 0.030 m, respectively. Compared with ECOM7 and ECOM9 SRP models, the ECOM5 SRP model has worse orbit prediction accuracies during the eclipse seasons.

Author Contributions: Methodology, R.L. and C.Z.; software, H.M. and J.W.; validation, Y.Z. and G.Y.; investigation, J.W.; writing—original draft preparation, R.L.; writing—review and editing, J.W. and H.Y.; visualization, H.M.; supervision, J.W., Y.Z., G.Y. and H.Z. All authors have read and agreed to the published version of the manuscript.

Funding: This work was supported by State Key Laboratory of Geo-Information Engineering and Key Laboratory of Surveying and Mapping Science and Geospatial Information Technology of MNR, CASM (No. 2021-01-07, 2022-01-09), the National Natural Science Foundation of China (No. 42122026, 42174033, 42074043, 42174038), Youth Innovation Promotion Association of Chinese Academy of Sciences (2022126), and Major Special Project of China's Second Generation Satellite Navigation System (JZX2B202012GG0110).

Data Availability Statement: Precise satellite orbit products can be found in ftp://cddis.gsfc.nasa.gov/pub/gps/products/. SLR observation data can be found in ftp://cddis.gsfc.nasa.gov/pub/slr/data/npt_crd/, all accessed on 17 January 2022.

Acknowledgments: The authors acknowledge the IGS MGEX and ILRS for providing the multi-GNSS and SLR tracking data.

Conflicts of Interest: The authors declare no conflict of interest.

References

1. Yang, Y.; Mao, Y.; Sun, B. Basic performance and future developments of BeiDou global navigation satellite system. *Satell. Navig.* **2020**, *1*, 1–8. [CrossRef]
2. Li, R.; Wang, N.; Li, Z.; Zhang, Y.; Wang, Z.; Ma, H. Precise orbit determination of BDS-3 satellites using B1C and B2a dual-frequency measurements. *GPS Solut.* **2021**, *25*, 1–14. [CrossRef]
3. Ma, H.; Zhao, Q.; Verhagen, S.; Psychas, D.; Liu, X. Assessing the performance of multi-GNSS PPP-RTK in the local area. *Remote Sens.* **2020**, *12*, 3343. [CrossRef]
4. Li, Z.; Wang, N.; Hernández-Pajares, M.; Yuan, Y.; Krankowski, A.; Liu, A.; Zha, J.; García-Rigo, A.; Roma-Dollase, D.; Yang, H. IGS real-time service for global ionospheric total electron content modeling. *J. Geod.* **2020**, *94*, 1–16. [CrossRef]
5. Ma, H.; Verhagen, S. Precise point positioning on the reliable detection of tropospheric model errors. *Sensors* **2020**, *20*, 1634. [CrossRef] [PubMed]
6. Li, K.; Zhou, X.; Guo, N.; Zhou, S. Effect of PCV and attitude on the precise orbit determination of Jason-3 satellite. *J. Appl. Geod.* **2022**, *16*, 143–150. [CrossRef]
7. Li, R.; Li, Z.; Wang, N.; Tang, C.; Ma, H.; Zhang, Y.; Wang, Z.; Wu, J. Considering inter-receiver pseudorange biases for BDS-2 precise orbit determination. *Measurement* **2021**, *177*, 109251. [CrossRef]
8. Wang, Z.; Li, Z.; Wang, L.; Wang, N.; Yang, Y.; Li, R.; Zhang, Y.; Liu, A.; Yuan, H.; Hoque, M. Comparison of the real-time precise orbit determination for leo between kinematic and reduced-dynamic modes. *Measurement* **2022**, *187*, 110224. [CrossRef]
9. Zhang, Y.; Li, Z.; Li, R.; Wang, Z.; Yuan, H.; Song, J. Orbital design of LEO navigation constellations and assessment of their augmentation to BDS. *Adv. Space Res.* **2020**, *66*, 1911–1923. [CrossRef]
10. Chen, Q.; Song, S.; Zhou, W. Accuracy Analysis of GNSS Hourly Ultra-Rapid Orbit and Clock Products from SHAO AC of iGMAS. *Remote Sens.* **2021**, *13*, 1022. [CrossRef]
11. Choi, K.K.; Ray, J.; Griffiths, J.; Bae, T.-S. Evaluation of GPS orbit prediction strategies for the IGS Ultra-rapid products. *GPS Solut.* **2013**, *17*, 403–412. [CrossRef]
12. Li, Y.; Gao, Y.; Li, B. An impact analysis of arc length on orbit prediction and clock estimation for PPP ambiguity resolution. *GPS Solut.* **2015**, *19*, 201–213. [CrossRef]

13. Geng, T.; Zhang, P.; Wang, W.; Xie, X. Comparison of ultra-rapid orbit prediction strategies for GPS, GLONASS, Galileo and BeiDou. *Sensors* **2018**, *18*, 477. [CrossRef] [PubMed]
14. Tang, C.; Hu, X.; Zhou, S.; Guo, R.; He, F.; Liu, L.; Zhu, L.; Li, X.; Wu, S.; Zhao, G. Improvement of orbit determination accuracy for Beidou navigation satellite system with two-way satellite time frequency transfer. *Adv. Space Res.* **2016**, *58*, 1390–1400. [CrossRef]
15. Zhou, S.; Hu, X.; Zhou, J.; Chen, J.; Gong, X.; Tang, C.; Wu, B.; Liu, L.; Guo, R.; He, F. Accuracy analyses of precise orbit determination and timing for COMPASS/Beidou-2 4GEO/5IGSO/4MEO constellation. In *China Satellite Navigation Conference (CSNC) 2013 Proceedings*; Springer: Berlin/Heidelberg, Germany, 2013.
16. Yan, X.; Liu, C.; Huang, G.; Zhang, Q.; Wang, L.; Qin, Z.; Xie, S. A Priori Solar Radiation Pressure Model for BeiDou-3 MEO Satellites. *Remote Sens.* **2019**, *11*, 1605. [CrossRef]
17. Wang, C.; Guo, J.; Zhao, Q.; Ge, M. Improving the Orbits of the BDS-2 IGSO and MEO Satellites with Compensating Thermal Radiation Pressure Parameters. *Remote Sens.* **2022**, *14*, 641. [CrossRef]
18. Zhao, Q.; Guo, J.; Wang, C.; Lyu, Y.; Xu, X.; Yang, C.; Li, J. Precise orbit determination for BDS satellites. *Satell. Navig.* **2022**, *3*, 1–24. [CrossRef]
19. Kaplan, E.D.; Hegarty, C. *Understanding GPS/GNSS: Principles and Applications*; Artech House: Norwood, MA, USA, 2017.
20. Li, X.; Hu, X.; Guo, R.; Tang, C.; Zhou, S.; Liu, S.; Chen, J. Orbit and positioning accuracy for new generation BeiDou satellites during the Earth eclipsing period. *J. Navig.* **2018**, *71*, 1069–1087. [CrossRef]
21. Rodriguez-Solano, C.; Hugentobler, U.; Steigenberger, P.; Allende-Alba, G. Improving the orbits of GPS block IIA satellites during eclipse seasons. *Adv. Space Res.* **2013**, *52*, 1511–1529. [CrossRef]
22. Duan, B.; Hugentobler, U.; Chen, J.; Selmke, I.; Wang, J. Prediction versus real-time orbit determination for GNSS satellites. *GPS Solut.* **2019**, *23*, 1–10. [CrossRef]
23. Xia, F.; Ye, S.; Chen, D.; Tang, L.; Wang, C.; Ge, M.; Neitzel, F. Advancing the Solar Radiation Pressure Model for BeiDou-3 IGSO Satellites. *Remote Sens.* **2022**, *14*, 1460. [CrossRef]
24. Pavlis, N.K.; Holmes, S.A.; Kenyon, S.C.; Factor, J.K. The development and evaluation of the Earth Gravitational Model 2008 (EGM2008). *J. Geophys. Res. Solid Earth* **2012**, *117*, B4. [CrossRef]
25. Standish, E. JPL Planetary and Lunar Ephemerides, DE405/LE405. JPL IOM 312. F-98_048. 1998; pp. 42–196. Available online: https://ssd.jpl.nasa.gov/ftp/eph/planets/bsp/ (accessed on 17 January 2022).
26. Petit, G.; Luzum, B. IERS Conventions. 2010, Bureau International des Poids et Mesures Sevres (France). Available online: https://www.iers.org/IERS/EN/Publications/TechnicalNotes/tn36.html (accessed on 17 January 2022).
27. Lyard, F.; Lefevre, F.; Letellier, T.; Francis, O. Modelling the global ocean tides: Modern insights from FES2004. *Ocean. Dyn.* **2006**, *56*, 394–415. [CrossRef]
28. Guo, F.; Li, X.; Zhang, X.; Wang, J. Assessment of precise orbit and clock products for Galileo, BeiDou, and QZSS from IGS Multi-GNSS Experiment (MGEX). *GPS Solut.* **2017**, *21*, 279–290. [CrossRef]
29. Beutler, G.; Brockmann, E.; Gurtner, W.; Hugentobler, U.; Mervart, L.; Rothacher, M.; Verdun, A. Extended orbit modeling techniques at the CODE processing center of the international GPS service for geodynamics (IGS): Theory and initial results. *Manuscr. Geod.* **1994**, *19*, 367–386.
30. Springer, T.; Beutler, G.; Rothacher, M. A new solar radiation pressure model for GPS satellites. *GPS Solut.* **1999**, *2*, 50–62. [CrossRef]
31. Yue, M.; Song, X.; Jia, X.; Ruan, R. Analysis about parameters selection strategy of ECOM solar radiation pressure model for BeiDou satellites. *Acta Geod. Cartogr. Sin.* **2017**, *46*, 1812.
32. Montenbruck, O.; Steigenberger, P.; Kirchner, G. GNSS satellite orbit validation using satellite laser ranging. In Proceedings of the ILRS Workshop Proceedings, Fujiyoshida, Japan, 11–15 November 2013.
33. Wang, C.; Guo, J.; Zhao, Q.; Liu, J. Yaw attitude modeling for BeiDou I06 and BeiDou-3 satellites. *GPS Solut.* **2018**, *22*, 1–10. [CrossRef]
34. Zhao, Q.; Wang, C.; Guo, J.; Wang, B.; Liu, J. Precise orbit and clock determination for BeiDou-3 experimental satellites with yaw attitude analysis. *GPS Solut.* **2018**, *22*, 1–13. [CrossRef]
35. Wang, W.; Chen, G.; Guo, S.; Song, X.; Zhao, Q. A Study on the Beidou IGSO/MEO Satellite Orbit Determination and Prediction of the Different Yaw Control Mode. In *China Satellite Navigation Conference (CSNC) 2013 Proceedings: Volume III. Lecture Notes in Electrical Engineering*; Springer: Berlin/Heidelberg, Germany, 2013; pp. 31–40.
36. Li, X.; Guo, R.; Wu, S.; Chang, Z.; Liu, S.; Chen, J. Orbit Determining Strategy Analysis for BeiDou Satellite in Different Attitude Control Modes. *Geomat. Inf. Sci. Wuhan Univ.* **2019**, *44*, 1465–1471.
37. Dai, X.; Ge, M.; Lou, Y.; Shi, C.; Wickert, J.; Schuh, H. Estimating the yaw-attitude of BDS IGSO and MEO satellites. *J. Geod.* **2015**, *89*, 1005–1018. [CrossRef]